

FedS2R: One-Shot Federated Domain Generalization for Synthetic-to-Real Semantic Segmentation in Autonomous Driving

Tao Lian¹ Jose L. Gómez¹ Antonio M. López^{1,2}

¹Computer Vision Center

²Department of Computer Science, Autonomous University of Barcelona (UAB)

{tlian, jlgomez, antonio}@cvc.uab.es

Abstract

Federated domain generalization has shown promising progress in image classification by enabling collaborative training across multiple clients without sharing raw data. However, its potential in the semantic segmentation of autonomous driving remains underexplored. In this paper, we propose FedS2R, the first one-shot federated domain generalization framework for synthetic-to-real semantic segmentation in autonomous driving. FedS2R comprises two components: an inconsistency-driven data augmentation strategy that generates images for unstable classes, and a multi-client knowledge distillation scheme with feature fusion that distills a global model from multiple client models. Experiments on five real-world datasets, Cityscapes, BDD100K, Mapillary, IDD, and ACDC, show that the global model significantly outperforms individual client models and is only 2 mIoU points behind the model trained with simultaneous access to all client data. These results demonstrate the effectiveness of FedS2R in synthetic-to-real semantic segmentation for autonomous driving under federated learning

1. Introduction

Semantic segmentation [5] is a key perception task in autonomous driving [11, 25], enabling pixel-wise understanding of road scenes. However, training such models typically requires large-scale datasets with precise pixel-level human annotations, which are expensive and labor-intensive processes. To avoid human annotation, many studies leverage synthetic datasets generated by computers that can automatically provide pixel-level annotations. Despite this advantage, the domain gap between synthetic and real-world data often results in poor generalization to unseen domains, restricting the practical deployment of synthetic-trained models. In addition, synthetic datasets [8, 22, 23, 27] are developed by academic or industrial entities using proprietary engines and assets. Several works utilize multi-source syn-

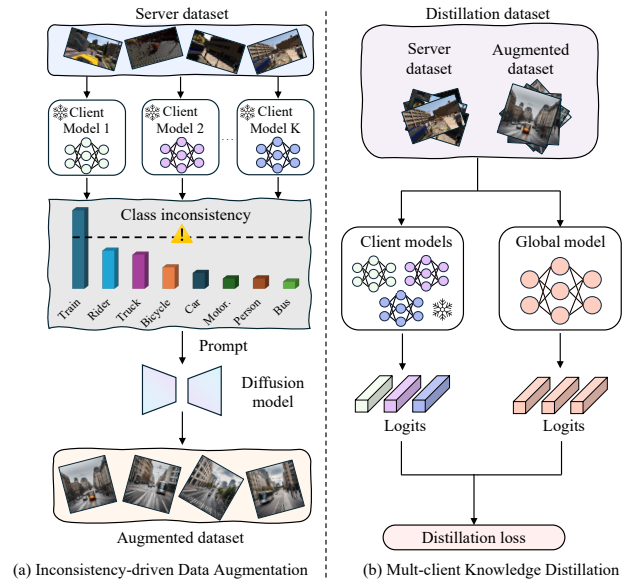


Figure 1. The proposed FedS2R consists of two stages: inconsistency-driven data augmentation using diffusion models to generate images for unstable classes; and (b) multi-client knowledge distillation to distill multiple client models into a global model. The star symbol (*) indicates that the model weights are frozen. Importantly, all client models are used for inference, and our framework does not require any annotations for the server dataset. Our framework is designed for the scenario where both clients and the server hold private datasets, and clients only send model weights, trained solely on their local dataset, to the server. The server then utilizes its own dataset (server dataset), along with the received client models, to train a global model.

thetic datasets [7, 8, 13] as a common strategy to improve results further, and even vision foundational models use synthetic datasets inside the massive amounts of data used to train them. Nevertheless, to protect intellectual property, dataset owners often enforce strict licensing agreements and prohibit the redistribution or unauthorized use of their datasets, particularly in commercial or sensitive do-

mains, such as those involving generative AI. Furthermore, to increase realism, some datasets incorporate identifiable geographic layouts or city-specific features [28], which can raise significant privacy and confidentiality concerns if shared without proper control. Consequently, unrestricted data sharing is often infeasible in practice, especially in autonomous driving scenarios where data is distributed across institutions or tied to proprietary geographic or sensor-specific information. For instance, an autonomous driving company with divisions around the world, where each team gathers its data and is subject to each country’s copyright laws. Data sharing between these divisions can be a burden, where a feasible solution would be to share trained models instead.

To address the domain gap and data privacy concerns, recent research has increasingly turned to federated domain generalization [1, 2, 6, 14, 32, 34], which integrates federated learning and domain generalization. This paradigm follows a client-server structure, where data remains local to the clients (e.g., companies or institutions that own the datasets), and only model weights or gradients are communicated with the server. This setup not only preserves data privacy but also aligns with practical constraints in scenarios where data sharing is legally or ethically restricted, while enabling the learning of domain-invariant representations. Current federated domain generalization research focuses on image classification [2, 9, 18, 29, 32, 34], with limited attention to semantic segmentation for autonomous driving. In addition, most of these works require multiple rounds of communication between the server and clients, where some actions are expected from the clients (e.g., update weights). Requiring actions from the clients is often impractical in real-world scenarios where data holders typically share model weights only once without the possibility to participate in iterative training. Recently, several studies [9, 29, 33] have explored one-shot federated learning for domain generalization, requiring only a single round of communication between clients and the server. However, these methods remain limited to classification tasks, and the semantic segmentation task has yet to be explored.

In this paper, we propose FedS2R, a novel one-shot federated domain generalization framework for semantic segmentation from synthetic to real domains, specifically tailored for autonomous driving scenarios. As is shown in Fig. 1, FedS2R consists of two stages: inconsistency-driven data augmentation and multi-client knowledge distillation. In the distillation stage, FedS2R leverages knowledge distillation [10, 15, 16] to aggregate multiple client models into a global model without accessing any client data. Moreover, the global model is trained using a distillation dataset (server dataset) in a fully unsupervised manner, relying only on the pseudo labels provided by the client models on this dataset. Note that this dataset does not need any annota-

tion, bringing flexibility and adaptability. In our scenario, we limit ourselves to synthetic data due to the synth-to-real domain gap challenge, but real-world data could be easily added. We adopt the state-of-the-art Mask2Former architecture [3], known for its robust performance in segmentation tasks, and assume each client provides models with this architecture. Following the aforementioned example of a company with facilities around the world, our approach mimics the situation where all the divisions are using the same state-of-the-art model to share weights. To the best of our knowledge, this is the first federated domain generalization framework designed for synthetic-to-real semantic segmentation in autonomous driving. It is also the first to distill multiple Mask2Former models into a single global model without requiring ground-truth for the distillation data. Experiments on five real-world datasets, Cityscapes, BDD100K [31], Mapillary [20], IDD [26], and ACDC [24], demonstrate that the distilled global model outperforms each client model individually and is only 2 mIoU points behind a trained global model with simultaneous access to all the data. Marking a significant contribution in federated domain generalization for semantic segmentation of autonomous driving. In summary, our contributions are threefold:

- We propose a novel federated domain generalization framework for semantic segmentation from synthetic to real domains for autonomous driving.
- We introduce transformer-based Mask2Former models into the federated domain generalization setting, demonstrating their feasibility and advantages.
- We achieve consistent generalization performance of the global model on multiple real-world datasets without requiring any ground-truth.

2. Related work

Federated Learning. Federated learning is a distributed client-server paradigm that enables multiple clients to collaboratively train a global model without sharing data. The most widely used algorithm, FedAvg [18], performs multiple communication rounds by aggregating client models on a central server and redistributing the global model back to the clients for further training. Subsequent works build on FedAvg, further improving the performance of image classification [2, 32, 34] and medical image segmentation [14]. In contrast, relatively fewer studies have focused on semantic segmentation. FedSeg [19] proposes a modified cross-entropy loss to address the foreground-background inconsistency caused by class heterogeneity in federated segmentation. ASAM [1] improves generalization by applying sharpness-aware minimization locally and averaging stochastic weights on the server to narrow the gap between federated and centralized models. FMTDA [30] tackles both server-client and inter-client domain shifts by for-

mutating a domain adaptation problem with one source and multiple target domains. Despite their contributions, these methods require multiple communication rounds and re-training on the client side, introduce significant communication overhead, client dependency, and deployment complexity.

To reduce communication overhead and client dependency, one-shot federated learning has emerged as an alternative, requiring only a single round of weight upload from clients. DENSE [33] introduces a two-stage framework involving data generation and model distillation to train a global model without accessing client data or performing client retraining. FedDEO [29] learns client-specific descriptions to guide diffusion models in generating synthetic data to train the global model. FedCVAE [9] trains conditional VAEs on each client, then leverages the uploaded decoders and label distributions on the server side to generate synthetic samples for training the global model. Although these one-shot methods effectively reduce communication costs via knowledge distillation, they primarily target image classification. In this work, we explore a one-shot federated setting on semantic segmentation, especially relevant for the autonomous driving community due to concerns about data privacy.

Federated Domain Generalization. Federated domain generalization integrates federated learning and domain generalization to train models across decentralized domains without data sharing. This paradigm is particularly well-suited for scenarios where data centralization is infeasible due to privacy, legal, or storage constraints. Although federated domain generalization has gained attention in image classification [1, 2, 32, 34], semantic segmentation remains underexplored. FedDrive [6] introduces a benchmark for semantic segmentation under federated domain generalization. However, it evaluates performance across different cities within the Cityscapes dataset, undermining the domain generalization. It also employs a lightweight model and the standard FedAvg communication strategy, which limits its applicability in real-world scenarios where more powerful architectures and one-shot communication settings are typically required. Furthermore, in synthetic-to-real domains in federated learning, DDI [17] constructs clients with mixed distributions from GTA5 and Cityscapes to study a synthetic-plus-real to real setting. Moreover, most segmentation-oriented federated learning frameworks [6, 19] assume homogeneous data between clients (e.g., partitions of the same dataset), whereas real-world federated setups often involve heterogeneous domains. This discrepancy is especially pronounced in synthetic-to-real scenarios, where client models trained on different synthetic datasets face significant domain gaps. Our work addresses federated domain generalization for semantic segmentation under a synthetic-to-real setting, where each client is trained on a

separate synthetic dataset.

3. Method

In this section, we present our framework, FedS2R, which comprises two main components: (1) inconsistency-driven data augmentation to identify and synthesize unstable classes, and (2) multi-client knowledge distillation with feature-level alignment and class-mask-level loss to train a robust global model. Prior studies [2, 6, 18, 34] generally adopt lightweight architectures, resulting in constrained representational capacity and suboptimal performance for the semantic segmentation task. Thus, we adopt the high-capacity Mask2Former for both clients and the server to capture complex scene semantics more accurately. Moreover, FedS2R follows a one-shot federated setting, where each client uploads its model weights only once, making the framework more practical for real-world deployment in privacy-sensitive applications.

3.1. Problem Formulation

Assume there are K clients and a server. Each client holds a private dataset $\mathcal{D}_K = \{x_k^i, y_k^i\}_{i=1}^{N_K}$ covering C classes, while the server has no access to any raw client data. Each client trains a local segmentation model f_k on its dataset and uploads the model weights to the server. The server maintains a separate dataset $\mathcal{D}_G = \{x_i\}_{i=1}^{N_G}$ as server dataset. The objective is to train a global model f_G to predict the same C classes and outperform individual client models on unseen real domains, under data privacy constraints and without requiring access to target domain data. Furthermore, f_G needs to be as close as possible to a global model trained with unrestricted access to all the data, considered our upper-bound.

3.2. Inconsistency-driven Data Augmentation

We assume each client model is independently trained on a different dataset. Due to varying class distributions across client datasets, client models often yield inconsistent predictions on the same image, particularly for unbalanced or inconsistent classes. Moreover, the server dataset \mathcal{D}_G may also exhibit class imbalance, which can lead to instability in training the global model. Both issues can hinder the effectiveness of the distilled global model.

To address this issue, we introduce an *inconsistency-driven data augmentation* strategy that quantifies class-level prediction inconsistency to identify unstable classes and employs a diffusion model to generate additional images for these classes. The detailed procedure is illustrated in Figs. 2 and implemented in Algorithm 1. First, we use client models f_k to make predictions $\hat{y}_i^k \in [0, 1, \dots, C - 1]$ for images x_i in \mathcal{D}_G . Since the most relevant objects for autonomous driving that normally suffer from imbalance are

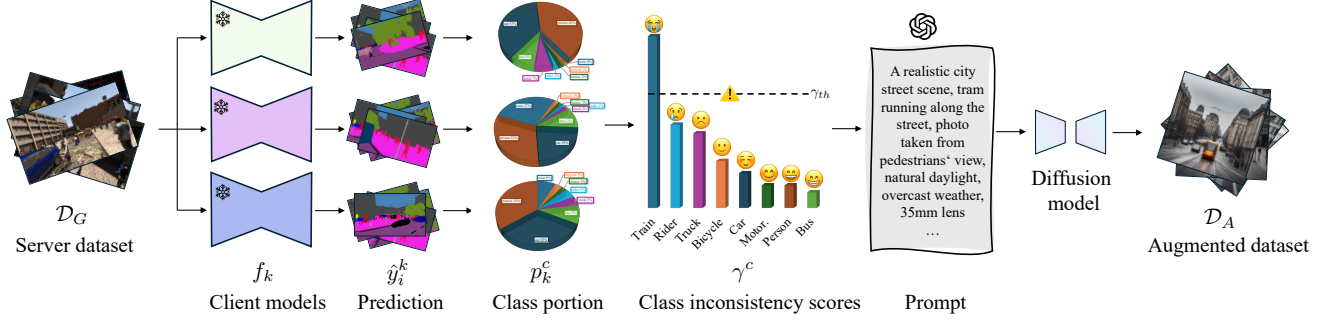


Figure 2. Overview of the inconsistency-driven data augmentation strategy. The strategy first employs client models to make predictions on the server dataset and calculates class-level inconsistency scores based on the class portions to identify unstable classes. Subsequently, prompts related to these unstable classes are generated using ChatGPT, and a diffusion model is used to synthesize corresponding images.

Algorithm 1 Inconsistency-Driven Augmentation

Input: Server dataset \mathcal{D}_G , client models $\{f_k\}_{k=1}^K$, dynamic foreground class set \mathcal{M} , threshold γ_{th}

Output: Augmented dataset \mathcal{D}_A

```

1: Initialize matrix  $\mathbf{R} \in \mathbb{R}^{K \times |\mathcal{M}|}$ 
2: for each image  $x_i \in \mathcal{D}_G$  do
3:   for each client  $k$  do
4:     Predict pseudo-label  $\hat{y}_i^k = f_k(x_i)$ 
5:     Initialize class count vector  $N_k \in \mathbb{R}^{|\mathcal{M}|}$ 
6:     for each class  $c \in \mathcal{M}$  do
7:       Count  $N_k^c \leftarrow$  pixels in  $\hat{y}_i^k$  labeled  $c$ 
8:     end for
9:     Normalize and update  $\mathbf{R}[k, :] \leftarrow \text{Softmax}(N_k)$ 
10:  end for
11: end for
12: Compute mean  $\mu^c$ , std  $\sigma^c$ , and inconsistency score  $\gamma^c$ 
13: Select  $\mathcal{R} = \{c \mid \gamma^c > \gamma_{th}\}$ 
14: for each class  $c \in \mathcal{R}$  do
15:   Generate scene-aware prompt  $p_c$  via LLM
16:   for  $n = 1$  to  $N$  do
17:      $\mathcal{D}_A \leftarrow \text{Diffusion}(p_c)$ 
18:   end for
19:   Construct distillation set:  $\mathcal{D}_{GA} \leftarrow \mathcal{D}_G \cup \mathcal{D}_A$ 
20: end for
```

the dynamic ones, we select a subset with dynamic foreground classes $\mathcal{M} \subseteq [0, 1, \dots, C-1]$ to be considered in the inconsistency analysis. For each client k and class $c \in \mathcal{M}$, we calculate the relative class proportion as:

$$p_k^c = \frac{N_k^c}{\sum_{c \in \mathcal{M}} N_k^c}, \quad (1)$$

where N_k^c denotes the number of pixels predicted as class c by the client k across all images in \mathcal{D}_G . This proportion reflects the relative frequency of class c among class set \mathcal{M} . To quantify class inconsistency scores across clients,

we compute the mean and standard deviation of each class proportion as follows:

$$\mu^c = \frac{1}{K} \sum_{k=1}^K p_k^c, \quad \sigma^c = \sqrt{\frac{1}{K} \sum_{k=1}^K (p_k^c - \mu^c)^2}. \quad (2)$$

We then define the inconsistency score γ^c as:

$$\gamma^c = \frac{\sigma^c}{\mu^c + \epsilon} \quad (3)$$

where ϵ is a small constant to ensure numerical stability. A higher γ^c indicates either a low class presence or high disagreement across clients, suggesting this class is unstable. Based on this score, we define the unstable class set \mathcal{R} as $\mathcal{R} = \{c \in \mathcal{M} \mid \gamma^c > \gamma_{th}\}$, where γ_{th} is a threshold. For each class $c \in \mathcal{R}$, we use a large language model (e.g., ChatGPT) to generate semantically descriptive prompts tailored to autonomous driving scenes. These prompts are fed into a pre-trained diffusion model to synthesize diverse and photorealistic images containing class c . The distillation dataset \mathcal{D}_{GA} is constructed by combining the server dataset \mathcal{D}_G with the augmented dataset \mathcal{D}_A produced by the diffusion model $\mathcal{D}_{GA} = \mathcal{D}_G \cup \mathcal{D}_A$. This strategy enhances the representation of unstable classes in the server dataset while preserving the privacy-aware and annotation-free nature of the framework.

3.3. Multi-client Feature Fusion and Distillation

Following the inconsistency-driven strategy, we perform knowledge distillation to transfer information from client models $\{f_k\}_{k=1}^K$ to a global model f_G . Each client model f_k follows the Mask2Former architecture and comprises a backbone B_k , a pixel decoder H_k^p , and a transformer decoder H_k^t . The global model f_G deployed on the server adopts the same architecture. The procedure is illustrated in Fig. 3 and implemented in Algorithm 2. Given an image

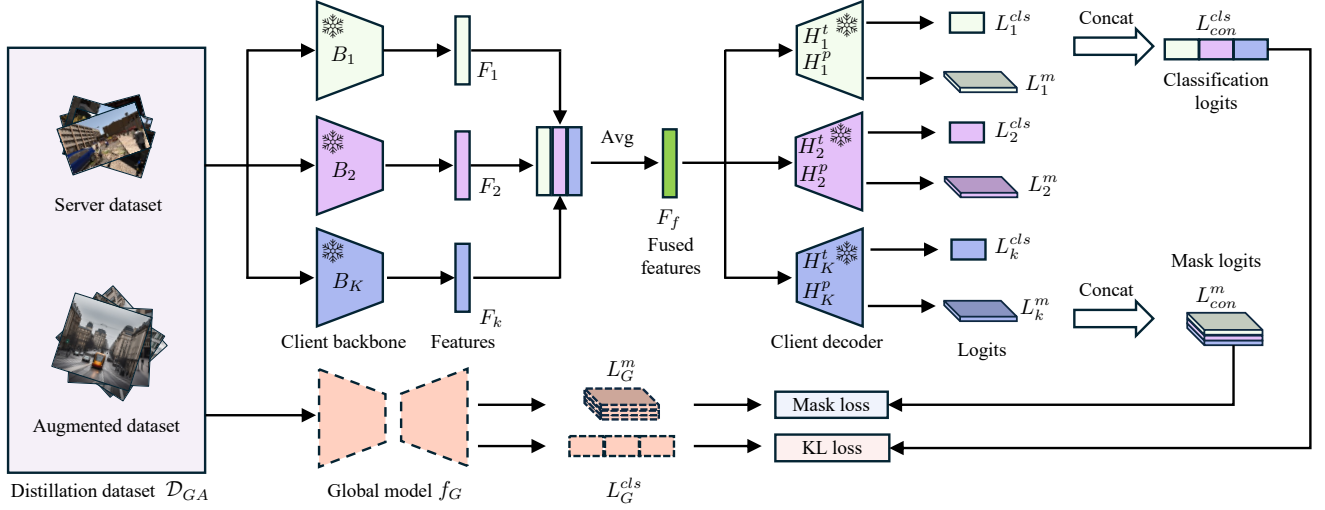


Figure 3. Overview of multi-client distillation with feature fusion. Client models extract backbone features, which are averaged and passed through the decoder to produce classification and mask logits. These logits are then respectively concatenated across clients and used to compute the distillation loss with the corresponding logits from the global model.

Algorithm 2 Multi-client Feature Fusion and Distillation

Input: Distillation dataset \mathcal{D}_{GA} , client models $\{f_k = (B_k, H_k^t, H_k^p)\}_{k=1}^K$, untrained global model f_G

Output: Trained global model f_G

- 1: Set learning rate η , loss weight λ_{cls} , λ_m
- 2: **for** minibatch $x \in \mathcal{D}_{GA}$ **do**
- 3: **for** $k = 1$ to K **do**
- 4: Client backbone features: $F_k \leftarrow B_k(x)$
- 5: **end for**
- 6: Fuse features: $F_f \leftarrow \frac{1}{K} \sum_{k=1}^K F_k$
- 7: **for** $k = 1$ to K **do**
- 8: Classification logits: $L_k^{cls} \leftarrow H_k^t(F_f)$
- 9: Mask logits: $L_k^m \leftarrow H_k^p(F_f)$
- 10: **end for**
- 11: Concatenate: $L_{con}^{cls} \leftarrow \text{Concat}(L_k^{cls})$
- 12: Concatenate: $L_{con}^m \leftarrow \text{Concat}(L_k^m)$
- 13: Global model logits: $L_G^{cls}, L_G^m \leftarrow f_G(x)$
- 14: $\mathcal{L}_{cls} \leftarrow KL(L_{con}^{cls}, L_G^{cls})$
- 15: $\mathcal{L}_m \leftarrow BCE(L_{con}^m, L_G^m) + \text{Dice}(L_{con}^m, L_G^m)$
- 16: Total loss: $\mathcal{L}_{total} \leftarrow \lambda_{cls} \cdot \mathcal{L}_{cls} + \lambda_m \cdot \mathcal{L}_m$
- 17: Update global model: $\theta \leftarrow \theta - \eta \cdot \nabla_{\theta} \mathcal{L}_{total}$
- 18: **end for**

$x \in \mathcal{D}_{GA}$, with $x \in \mathbb{R}^{3 \times H \times W}$, each client backbone B_k extracts intermediate feature maps as:

$$F_k = B_k(x) \in \mathbb{R}^{C_f \times H' \times W'}, \quad (4)$$

where C_f denotes the number of feature channels, and H' , W' represent the downsampled spatial dimensions. Since client models are trained on heterogeneous datasets, the ex-

tracted features F_k may capture different semantic cues. To integrate these diverse representations, we perform feature-level fusion by averaging features from all client backbones:

$$F_f = \frac{1}{K} \sum_{k=1}^K F_k \in \mathbb{R}^{C_f \times H' \times W'}. \quad (5)$$

The fused features are then passed through the decoders of each client to produce classification logits L_k^{cls} and mask logits L_k^m :

$$\begin{aligned} L_k^{cls} &= H_k^t(F_f) \in \mathbb{R}^{Q \times (C+1)} \\ L_k^m &= H_k^p(F_f) \in \mathbb{R}^{Q \times H' \times W'}, \end{aligned} \quad (6)$$

where Q is the number of object queries and $C+1$ includes an additional background class. Although all client models are trained on datasets with the same class space C , the object queries in Mask2Former are randomly initialized and do not possess fixed semantic associations. Consequently, query indices are not aligned across models, i.e., query q in client A may attend to entirely different classes or spatial regions than the same index q in client B . This lack of semantic correspondence makes it infeasible to directly compare or aggregate query-level logits across clients in a federated setting. Although inspired by [12], which relies on ground-truth labels for bipartite matching between student and teacher models, we adopt a label-free strategy by equally aggregating all query outputs, without requiring any ground-truth-based matching. Specifically, we concatenate classification logits L_k^{cls} and mask logits L_k^m from all clients

individually:

$$\begin{aligned} L_{con}^{cls} &= \text{Concat}(L_1^{cls}, \dots, L_K^{cls}) \in \mathbb{R}^{KQ \times (C+1)} \\ L_{con}^m &= \text{Concat}(L_1^m, \dots, L_K^m) \in \mathbb{R}^{KQ \times H' \times W'}, \end{aligned} \quad (7)$$

Then, the global model f_G processes the same image x to generate its own classification logits $L_G^{cls} \in \mathbb{R}^{KQ \times (C+1)}$ and mask logits $L_G^m \in \mathbb{R}^{KQ \times H' \times W'}$. In Mask2Former, classification and mask logits collectively determine the final segmentation output. To effectively distill the knowledge learned by client models into the global model, we apply two types of loss: classification distillation loss and mask distillation loss. For classification, we use temperature-scaled Kullback-Leibler (KL) divergence as classification distillation loss:

$$\begin{aligned} \mathbf{p}_c^q &= \log \left(\text{Softmax} \left(\frac{L_{con}^{cls,q}}{\tau} \right) \right) \in \mathbb{R}^C \\ \mathbf{q}_c^q &= \text{Softmax} \left(\frac{L_G^{cls,q}}{\tau} \right) \in \mathbb{R}^C \\ \mathcal{L}_{cls} &= \frac{1}{KQ} \sum_{q=1}^{KQ} \sum_{c=1}^C p_c^q \log \left(\frac{p_c^q}{q_c^q} \right), \end{aligned} \quad (8)$$

where τ is a temperature scaling parameter and q indexes the object query. The KL divergence loss encourages the global model to align with the probabilistic output distributions (i.e., soft predictions) of the client models, enabling it to capture the class-level knowledge in their predictions. For the mask distillation loss \mathcal{L}_m , we combine binary cross-entropy (BCE) and Dice loss:

$$\mathcal{L}_m = \text{BCE}(L_G^m, L_{con}^m) + \text{Dice}(L_G^m, L_{con}^m). \quad (9)$$

While BCE loss enforces pixel-wise consistency between global and client predictions, Dice loss emphasizes region-level overlap quality, particularly beneficial for handling small or imbalanced foreground regions. The total loss used to train the global model is a weighted sum of the classification and mask losses:

$$\mathcal{L}_{total} = \lambda_{cls} \cdot \mathcal{L}_{cls} + \lambda_m \cdot \mathcal{L}_m, \quad (10)$$

where λ_{cls} and λ_m are weight coefficients for each loss.

4. Experiments

4.1. Datasets

We establish our federated domain generalization setting using four synthetic datasets: GTA5 [22], Synscapes [27], UrbanSyn [8], and Synthia [23]. These datasets employ different rendering technologies, leading to variations in image quality and coverage of distinct driving scenarios. Specifically, GTA5 contains 24,966 images at a resolution of 1914×1052 ; Synscapes includes 25,000 images at 1440×720 ; UrbanSyn comprises 7,539 images

at 2048×1024 ; and Synthia provides 7,520 images rendered at 1280×760 . The synthetic datasets are distributed across three clients, with each client retaining one dataset locally. The remaining dataset is allocated to the server and serves as the knowledge distillation set. To evaluate the generalization performance of our method, we adopt five real-world semantic segmentation benchmarks as unseen target domains: Cityscapes [4], BDD100K [31], Mapillary [20], IDD [26], and ACDC [24]. Cityscapes consists of 2,975 training and 500 validation images at a resolution of 2048×1024 . BDD100K includes 7,000 training and 1,000 validation images at 1280×720 . Mapillary Vistas contains 18,000 training and 2,000 validation images with varying resolutions. IDD provides 6,993 finely annotated training images and 981 validation images at 1920×1080 . ACDC comprises 1,600 training and 400 validation images at 1920×1080 , captured under challenging conditions such as night, rain, and fog. All experiments are evaluated using the mean Intersection over Union (mIoU) computed across all semantic classes.

4.2. Implementation details

Client models. Each client employs the Mask2Former architecture with a Swin-Large backbone pre-trained on ImageNet-21K. Input images are randomly cropped to a resolution of 1024×512 . Training is conducted using the AdamW optimizer with a learning rate of 1×10^{-4} , a batch size of 2, and 100 object queries over 90,000 iterations. All other hyperparameters follow the official Mask2Former configuration.

Global model. The global model adopts the Mask2Former architecture with a Swin-Large backbone pre-trained on ImageNet-21K, and operates at an input resolution of 1024×512 . To ensure compatibility with the concatenated outputs from multiple client models, the number of object queries in the global model is set to 300, matching the total number of queries aggregated from the $K = 3$ client models (each with 100 queries). The optimization settings mirror those of the client models, employing the AdamW optimizer with a learning rate of 1×10^{-4} . The temperature parameter for KL divergence is set to $\tau = 1.0$, and both loss terms are weighted equally with $\lambda_{cls} = \lambda_{mask} = 1.0$.

Inconsistency-driven Augmentation. We apply our inconsistency-driven augmentation strategy to eight dynamic foreground classes: *person*, *rider*, *car*, *truck*, *bus*, *train*, *motorcycle*, and *bicycle*. The inconsistency score threshold is set to 1.0. For each selected class, we generate 100 high-quality images using the Stable Diffusion XL (SDXL) pipeline [21]. Both the base model and the refiner are employed: the base model runs for 40 inference steps with a guidance scale of 7.5, followed by 20 refinement steps under the same guidance. To ensure semantic alignment with driving scenes, class-specific prompts are

Method	Dataset				mIoU					
	Client 1	Client 2	Client 3	Server	Cityscapes	BDD100K	Mapillary	IDD	ACDC	Average
Baseline	-	-	-	GTA5	56.9	49.2	62.6	53.8	46.0	53.7
	-	-	-	Synscapes	54.0	38.8	55.2	46.1	40.3	46.9
	-	-	-	Urbansyn	63.9	44.9	60.0	49.6	40.9	51.9
	-	-	-	Synthia	43.0	34.5	41.7	32.0	30.7	36.4
	-	-	-	GSUS	68.6	55.5	68.0	58.3	53.2	60.7
FedAvg	GTA5	Synscapes	Urbansyn	Synthia	45.0	34.9	42.8	33.3	30.2	37.2
Ours	GTA5	Synscapes	Urbansyn	Synthia	67.9	53.1	65.1	56.5	49.8	58.5
FedAvg	GTA5	Synscapes	Synthia	Urbansyn	67.0	46.2	62.6	51.7	42.1	53.9
Ours	GTA5	Synscapes	Synthia	Urbansyn	64.0	53.9	65.8	55.9	52.5	58.4
FedAvg	GTA5	Synthia	Urbansyn	Synscapes	56.8	39.8	56.9	46.5	42.6	48.5
Ours	GTA5	Synthia	Urbansyn	Synscapes	64.9	54.8	66.2	57.6	48.3	58.4
FedAvg	Synthia	Synscapes	Urbansyn	GTA5	64.1	50.2	63.2	53.4	47.6	55.7
Ours	Synthia	Synscapes	Urbansyn	GTA5	64.6	50.8	63.5	53.2	47.8	56.0

Table 1. Performance of FedAvg and Ours under various client-server dataset configurations. “Baseline” denotes a centralized setting where the server is allowed to access all client data for direct training. “GSUS” refers to the merged dataset consisting of GTA5, Synscapes, UrbanSyn, and Synthia and represents our upper-bound.

Method	Server	IoU																			mIoU
		Road	S.walk	Build	Wall	Fence	Pole	Tr. Light	Tr. Sign	Vege.	Terrain	Sky	Person	Rider	Car	Truck	Bus	Train	M.cycle	Bicycle	
Baseline	GTA5	85.1	36.8	89.2	40.2	47.5	47.6	59.6	44.6	89.9	41.5	89.9	76.4	41.8	90.2	50.2	63.0	19.9	35.7	32.0	56.9
	Synscapes	89.4	47.9	75.5	36.2	34.0	55.0	52.7	64.3	89.0	44.6	93.9	70.2	32.9	89.9	33.5	16.9	5.0	32.9	61.8	54.0
	Urbansyn	88.6	48.1	89.6	28.0	54.4	60.1	63.0	74.0	89.6	48.5	92.6	79.5	58.4	91.7	55.7	55.2	33.0	32.9	71.5	63.9
	Synthia	78.3	36.6	86.1	22.4	2.2	54.4	50.2	39.1	85.7	0.0	86.5	71.2	22.5	84.2	0.0	18.9	0.0	37.8	40.6	43.0
	GSUS	91.7	58.2	91.1	55.8	57.6	63.2	66.0	74.2	91.4	53.9	94.5	80.2	55.0	93.2	57.9	65.0	40.6	42.6	70.5	68.6
FedAvg	Synthia	80.4	37.2	87.4	26.6	3.6	57.0	49.4	42.1	86.9	0.0	89.3	71.7	21.3	85.7	0.0	34.0	0.0	42.7	39.4	45.0
Ours		92.3	56.6	91.0	50.5	56.7	58.3	58.0	71.2	90.7	51.9	92.1	79.5	56.3	91.9	58.1	69.8	56.8	39.8	68.5	67.9
FedAvg	Urbansyn	90.3	53.0	90.2	36.4	56.1	63.0	64.6	74.5	89.8	50.3	93.1	80.2	57.8	94.2	55.1	66.8	50.7	34.2	72.4	67.0
Ours		91.6	55.7	90.5	43.9	49.2	60.4	64.4	58.1	91.0	49.8	92.8	76.0	37.9	92.3	68.9	63.9	15.9	52.7	60.7	64.0
FedAvg	Synscapes	89.5	51.0	81.3	40.7	38.9	57.5	54.5	68.1	89.8	51.1	93.8	71.8	33.2	89.9	39.3	25.1	6.5	34.1	62.0	56.8
Ours		91.5	53.9	90.9	48.3	47.8	58.0	64.4	61.0	91.1	48.9	92.1	80.0	55.0	93.5	79.2	64.7	4.7	45.6	62.8	64.9
FedAvg	GTA5	84.7	39.2	89.6	45.1	49.3	53.8	63.3	49.7	90.0	43.9	90.6	78.8	49.5	92.1	52.0	71.6	52.0	35.4	46.7	64.1
Ours		90.3	51.9	90.9	40.7	55.3	60.7	65.4	71.2	91.1	50.5	94.5	78.8	50.2	92.8	71.1	50.7	24.0	32.4	55.1	64.6

Table 2. Per-class IoU results on Cityscapes under different federated client-server dataset configurations.

automatically constructed via ChatGPT. Negative prompts are fixed as “cartoon, illustration, low quality, blurry, fantasy, surreal, painting” to encourage photorealistic generation. All generated images are rendered at a resolution of 1024×1024 and incorporated into the server-side distillation dataset.

4.3. Comparison with FedAvg

Tab. 1 presents the performance of our method on five real domains compared with FedAvg under various client-server configurations. Since there is no existing work addressing this scenario, we compare our method with the representative baseline FedAvg. Specifically, we evaluate the performance of FedAvg under a one-shot federated learning setting for fair comparison. Across all configurations, our method consistently outperforms FedAvg in the averaged mIoU of all target domains. For example, when client datasets are GTA5, Synscapes, and UrbanSyn, and the server is Synthia, our method achieves an mIoU of 58.5, significantly outperforming FedAvg. This result is only 2.2 points below the upper-bound GSUS (model trained with simultaneous access to all datasets). Compared to baseline models trained individually on each client dataset, our method shows superior performance. Our method achieves

58.5 averaged mIoU, which is higher than any of the baselines: 53.7 for GTA5, 46.9 for Synscapes, and 51.9 for UrbanSyn. Besides the averaged mIoU, our method also outperforms baseline models on target domains in specific cases. For example, it achieves 67.9 on Cityscapes, while baselines trained on GTA5, Synscapes, and UrbanSyn obtain 56.9, 54.0, and 63.9, respectively. This highlights the effectiveness of our framework in integrating knowledge across clients without access to client data. Besides quantitative results, we present visualisations in Fig. 4 to illustrate the improvement of our framework.

Tab. 2 presents the per-class IoU results on the Cityscapes dataset across the same federated configurations of Tab. 1. In most settings, our method consistently outperforms FedAvg. For Synthia as the server dataset, our method achieves a mIoU of 67.9, with a 22.9 points improvement over FedAvg. Notable gains are observed in several classes such as *road* (92.3 vs 80.4), *sidewalk* (56.6 vs 37.2), *terrain* (51.9 vs 0), and *train* (58.1 vs 0). An exception occurs in the UrbanSyn configuration; our method yields a mIoU of 64.0, which is lower than the 67.0 achieved by FedAvg. This performance gap is largely attributable to the high quality of the UrbanSyn dataset (note that the Ur-

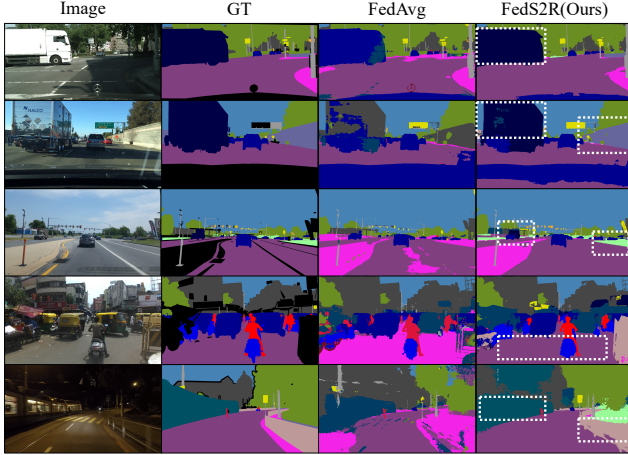


Figure 4. Qualitative comparisons between FedS2R and FedAvg under the configuration where Synthia serves as the server dataset. Rows 1–5 correspond to Cityscapes, BDD100K, Mapillary, IDD, and ACDC, respectively. FedS2R not only improves foreground classes such as *train* and *truck*, but also enhances background classes, including *road*, *terrain*, and *fence*.

banSyn baseline is by far the best baseline on Cityscapes), as well as the fact that FedAvg requires labeled server data during training, which is an advantage during the training. Despite being behind, our method still improves the segmentation performance for several dynamic classes, such as *truck* (68.9 vs 55.1) and *motorcycle* (52.7 vs 34.2). Similarly, in the Synscapes configuration, our method improves the mIoU from 56.8 to 64.9, with particularly large gains in *bus* (64.7 vs 25.1) and *rider* (55.0 vs 33.2). When GTA5 serves as the server dataset, our method achieves a mIoU of 64.6, surpassing FedAvg by 0.5 points and offering improved segmentation for classes like *pole* (60.7 vs 53.8) and *truck* (71.1 vs 52.0). These results demonstrate that our framework consistently matches or exceeds the performance of FedAvg across a broad range of class types, including both background classes (e.g., *building*, *road*) and dynamic foreground classes (e.g., *truck*, *bus*, *train*) without the necessity of labeled server data.

4.4. Ablation study

Components Tab. 3 presents the ablation study evaluating the contribution of each component in our proposed framework under the configuration of Synthia as the server dataset. Using KL loss in combination with BCE loss yields an averaged mIoU of 55.3. However, replacing BCE loss with Dice loss results in a substantial drop to 26.0. This performance degradation suggests that Dice loss alone is insufficient for effectively supervising mask prediction in our federated setting. While Dice loss emphasizes region-level overlap, it provides limited guidance for learning accurate mask boundaries and shapes, which are more effec-

Feature fusion	Inconsistency augmentation	Loss			Avg mIoU
		KL	Bce	Dice	
-	-	✓	✓	-	55.3
-	-	✓	-	✓	26.0
-	-	✓	✓	✓	56.4
✓	-	✓	✓	✓	57.1
-	✓	✓	✓	✓	57.2
✓	✓	✓	✓	✓	58.5

Table 3. Ablation of components of FedS2R under the configuration of Synthia as the server dataset.

Samples	10	100	500	1000
Avg mIoU	57.9	58.5	58.7	58.5

Table 4. Performance with varying numbers of generated images, using Synthia as the server dataset. Avg mIoU refers to the average of mIoU across five target domains.

tively captured by BCE loss. For feature fusion, which contributes an additional 0.7 points in averaged mIoU (from 56.4 to 57.1). This indicates that fusing features from client models facilitates the alignment of shared features across domains, which contributes to improved generalization. Adding inconsistency augmentation alone (without feature fusion) improves the averaged mIoU from 56.4 to 57.2 compared to the baseline. When combined with feature fusion, the full framework achieves the best performance (58.5). In summary, each component contributes meaningfully to the overall performance, and their combination leads to the best generalization across diverse and challenging target domains.

Quantity of generated images. Tab. 4 presents the performance of varying quantities of generated images using Synthia as the server dataset. The class *train* is selected as the unstable class for image generation since its inconsistency score exceeds the threshold. Performance initially improves with more generated samples, but slightly drops at 1000 due to noise and errors introduced by the diffusion model. As performance plateaus after 100 samples, we set the number of generated images to 100.

5. Conclusion

This paper proposes FedS2R, the first one-shot federated domain generalization framework for synthetic-to-real semantic segmentation in autonomous driving. FedS2R combines inconsistency-driven data augmentation and multi-client knowledge distillation with feature fusion. Extensive experiments on five real-world datasets, Cityscapes, BDD100K, Mapillary, IDD, and ACDC, show that the global model trained by our framework consistently outperforms all individual client models and performs only 2 mIoU points behind the model trained with simultaneous access to all client data. These results highlight the effectiveness and promise of federated domain general-

ization for semantic segmentation in autonomous driving.

References

- [1] Debora Caldarola, Barbara Caputo, and Marco Ciccone. Improving generalization in federated learning by seeking flat minima. In *European Conference on Computer Vision*, pages 654–672. Springer, 2022. 2, 3
- [2] Junming Chen, Meirui Jiang, Qi Dou, and Qifeng Chen. Federated domain generalization for image recognition via cross-client style transfer. In *Proceedings of the IEEE/CVF Winter Conference on Applications of Computer Vision*, pages 361–370, 2023. 2, 3
- [3] Bowen Cheng, Ishan Misra, Alexander G Schwing, Alexander Kirillov, and Rohit Girdhar. Masked-attention mask transformer for universal image segmentation. In *Proceedings of the IEEE/CVF conference on computer vision and pattern recognition*, pages 1290–1299, 2022. 2
- [4] Marius Cordts, Mohamed Omran, Sebastian Ramos, Timo Rehfeld, Markus Enzweiler, Rodrigo Benenson, Uwe Franke, Stefan Roth, and Bernt Schiele. The Cityscapes dataset for semantic urban scene understanding. In *CVPR*, 2016. 6
- [5] Gabriela Csurka, Riccardo Volpi, Boris Chidlovskii, et al. Semantic image segmentation: Two decades of research. *Foundations and Trends® in Computer Graphics and Vision*, 14(1-2):1–162, 2022. 1
- [6] Lidia Fantauzzo, Eros Fanì, Debora Caldarola, Antonio Tavera, Fabio Cermelli, Marco Ciccone, and Barbara Caputo. Feddrive: Generalizing federated learning to semantic segmentation in autonomous driving. In *2022 IEEE/RSJ International Conference on Intelligent Robots and Systems (IROS)*, pages 11504–11511. IEEE, 2022. 2, 3
- [7] Jose L Gómez, Gabriel Villalonga, and Antonio M López. Co-training for unsupervised domain adaptation of semantic segmentation models. *Sensors*, 23(2):621, 2023. 1
- [8] Jose L Gómez, Manuel Silva, Antonio Seoane, Agnès Borrás, Mario Noriega, Germán Ros, Jose A Iglesias-Guitián, and Antonio M López. All for one, and one for all: Urbansyn dataset, the third musketeer of synthetic driving scenes. *Neurocomputing*, 637:130038, 2025. 1, 6
- [9] Clare Elizabeth Heinbaugh, Emilio Luz-Ricca, and Huajie Shao. Data-free one-shot federated learning under very high statistical heterogeneity. In *The Eleventh International Conference on Learning Representations*, 2023. 2, 3
- [10] Geoffrey Hinton, Oriol Vinyals, and Jeff Dean. Distilling the knowledge in a neural network. *arXiv preprint arXiv:1503.02531*, 2015. 2
- [11] Joel Janai, Fatma Güney, Aseem Behl, Andreas Geiger, et al. Computer vision for autonomous vehicles: Problems, datasets and state of the art. *Foundations and trends® in computer graphics and vision*, 12(1–3):1–308, 2020. 1
- [12] Maohui Li, Michael Halstead, and Chris McCool. Knowledge distillation for efficient instance semantic segmentation with transformers. In *Proceedings of the IEEE/CVF Conference on Computer Vision and Pattern Recognition*, pages 5432–5439, 2024. 5
- [13] Tao Lian, Jose L Gómez, and Antonio M López. Divide, ensemble and conquer: The last mile on unsupervised domain adaptation for semantic segmentation. *IEEE Transactions on Intelligent Vehicles*, 2024. 1
- [14] Quande Liu, Cheng Chen, Jing Qin, Qi Dou, and Pheng-Ann Heng. Feddg: Federated domain generalization on medical image segmentation via episodic learning in continuous frequency space. In *Proceedings of the IEEE/CVF conference on computer vision and pattern recognition*, pages 1013–1023, 2021. 2
- [15] Yufan Liu, Jiajiong Cao, Bing Li, Chunfeng Yuan, Weiming Hu, Yangxi Li, and Yunqiang Duan. Knowledge distillation via instance relationship graph. In *Proceedings of the IEEE/CVF Conference on Computer Vision and Pattern Recognition*, pages 7096–7104, 2019. 2
- [16] Yifan Liu, Ke Chen, Chris Liu, Zengchang Qin, Zhenbo Luo, and Jingdong Wang. Structured knowledge distillation for semantic segmentation. In *Proceedings of the IEEE/CVF conference on computer vision and pattern recognition*, pages 2604–2613, 2019. 2
- [17] Matthias Manthe, Carole Lartizien, and Stefan Duffner. Deep domain isolation and sample clustered federated learning for semantic segmentation. In *Joint European Conference on Machine Learning and Knowledge Discovery in Databases*, pages 369–385. Springer, 2024. 3
- [18] Brendan McMahan, Eider Moore, Daniel Ramage, Seth Hampson, and Blaise Agüera y Arcas. Communication-efficient learning of deep networks from decentralized data. In *Artificial intelligence and statistics*, pages 1273–1282. PMLR, 2017. 2, 3
- [19] Jiaxu Miao, Zongxin Yang, Leilei Fan, and Yi Yang. Fedseg: Class-heterogeneous federated learning for semantic segmentation. In *Proceedings of the IEEE/CVF conference on computer vision and pattern recognition*, pages 8042–8052, 2023. 2, 3
- [20] Gerhard Neuhold, Tobias Ollmann, Samuel Rota Bulò, and Peter Kontschieder. The Mapillary Vistas dataset for semantic understanding of street scenes. In *ICCV*, 2017. 2, 6
- [21] Dustin Podell, Zion English, Kyle Lacey, Andreas Blattmann, Tim Dockhorn, Jonas Müller, Joe Penna, and Robin Rombach. SDXL: Improving latent diffusion models for high-resolution image synthesis. In *The Twelfth International Conference on Learning Representations*, 2024. 6
- [22] Stephan R Richter, Vibhav Vineet, Stefan Roth, and Vladlen Koltun. Playing for data: Ground truth from computer games. In *ECCV*, 2016. 1, 6
- [23] Germán Ros, Laura Sellart, Joanna Materzyska, David Vázquez, and Antonio M. López. The SYNTHIA dataset: a large collection of synthetic images for semantic segmentation of urban scenes. In *CVPR*, 2016. 1, 6
- [24] Christos Sakaridis, Dengxin Dai, and Luc Van Gool. Acdc: The adverse conditions dataset with correspondences for semantic driving scene understanding. In *Proceedings of the IEEE/CVF international conference on computer vision*, pages 10765–10775, 2021. 2, 6
- [25] Ardi Tampuu, Tambet Matiisen, Maksym Semikin, Dmytro Fishman, and Naveed Muhammad. A survey of end-to-end

- driving: Architectures and training methods. *IEEE Transactions on Neural Networks and Learning Systems*, 33(4): 1364–1384, 2020. [1](#)
- [26] Girish Varma, Anbumani Subramanian, Anoop Namboodiri, Manmohan Chandraker, and CV Jawahar. Idd: A dataset for exploring problems of autonomous navigation in unconstrained environments. In *2019 IEEE winter conference on applications of computer vision (WACV)*, pages 1743–1751. IEEE, 2019. [2](#), [6](#)
- [27] Magnus Wrenninge and Jonas Unger. Synscapes: A photorealistic synthetic dataset for street scene parsing. arXiv preprint arXiv:1810.08705, 2018. [1](#), [6](#)
- [28] Yao Xu, Jixin Wei, Ting Mi, and Zhihua Chen. Data security in autonomous driving: Multifaceted challenges of technology, law, and social ethics. *World Electric Vehicle Journal*, 16(1):6, 2024. [2](#)
- [29] Mingzhao Yang, Shangchao Su, Bin Li, and Xiangyang Xue. Feddeo: Description-enhanced one-shot federated learning with diffusion models. In *Proceedings of the 32nd ACM International Conference on Multimedia*, pages 6666–6675, 2024. [2](#), [3](#)
- [30] Chun-Han Yao, Boqing Gong, Hang Qi, Yin Cui, Yukun Zhu, and Ming-Hsuan Yang. Federated multi-target domain adaptation. In *Proceedings of the IEEE/CVF winter conference on applications of computer vision*, pages 1424–1433, 2022. [2](#)
- [31] Fisher Yu, Haofeng Chen, Xin Wang, Wenqi Xian, Yingying Chen, Fangchen Liu, Vashisht Madhavan, and Trevor Darrell. BDD100K: A diverse driving dataset for heterogeneous multitask learning. In *CVPR*, 2020. [2](#), [6](#)
- [32] Xinhui Yu, Dan Wang, Martin J McKeown, and Z Jane Wang. Contrastive-enhanced domain generalization with federated learning. *IEEE Transactions on Artificial Intelligence*, 5(4):1525–1532, 2023. [2](#), [3](#)
- [33] Jie Zhang, Chen Chen, Bo Li, Lingjuan Lyu, Shuang Wu, Shouhong Ding, Chunhua Shen, and Chao Wu. Dense: Data-free one-shot federated learning. *Advances in Neural Information Processing Systems*, 35:21414–21428, 2022. [2](#), [3](#)
- [34] Ruipeng Zhang, Qinwei Xu, Jiangchao Yao, Ya Zhang, Qi Tian, and Yanfeng Wang. Federated domain generalization with generalization adjustment. In *Proceedings of the IEEE/CVF Conference on Computer Vision and Pattern Recognition*, pages 3954–3963, 2023. [2](#), [3](#)